

Annual Progress Report  
for the period  
May 1, 1991 – April 30, 1992  
(Prepared January 1992)

Stephen J. Sanders  
Francis W. Prosser  
(Co-Principal Investigators)

Department of Physics and Astronomy  
The University of Kansas  
Lawrence, Kansas 66045

Prepared for the  
U.S. Department of Energy  
under Grant No. DE-FG02-89ER40506

**MASTER**

**DISTRIBUTION OF THIS DOCUMENT IS UNLIMITED**

*Research in Heavy-ion Nuclear Physics*  
**DISCLAIMER**

This report was prepared as an account of work sponsored by an agency of the United States Government. Neither the United States Government nor any agency thereof, nor any of their employees, makes any warranty, express or implied, or assumes any legal liability or responsibility for the accuracy, completeness, or usefulness of any information, apparatus, product, or process disclosed, or represents that its use would not infringe privately owned rights. Reference herein to any specific commercial product, process, or service by trade name, trademark, manufacturer, or otherwise does not necessarily constitute or imply its endorsement, recommendation, or favoring by the United States Government or any agency thereof. The views and opinions of authors expressed herein do not necessarily state or reflect those of the United States Government or any agency thereof.

## Table of Contents

I. Introduction.....	2
II. Research Program.....	4
A. Fusion-fission in light nuclear systems.....	4
Global fission systematics for $40 \leq A_{cn} \leq 80$ .....	4
Symmetric fission of $^{56}\text{Ni}$ .....	6
Fusion-fission in the $^{29}\text{Si}+^{27}\text{Al}$ reaction.....	9
B. High-resolution Q-value measurement for the $^{24}\text{Mg}+^{24}\text{Mg}$ reaction.....	11
C. Heavy-ion reactions and limits to fusion.....	13
D. Hybrid MWPC-Bragg curve detector development.....	16
III. Collaborators.....	18
IV. Meetings and Research Trips.....	18
V. Personnel.....	18
VI. Reprints and Preprints.....	19

## I. Introduction.

Last year the research goals of our group continued to be focussed on the fusion-fission process in light nuclear systems and the nuclear structures related to this process. Part of this effort, where the systematics of the fission process in light systems is being developed, led to a paper this year on a model calculation of these yields. The emphasis of our program has now shifted further towards exploring the experimental signatures of this process that can be directly related to the structure of the strongly deformed nuclear configurations leading to fission. To facilitate these measurement we completed construction of a large acceptance gas counter during the year. We have also continued work on a proposal to look for evidence of a nuclear temperature limit to fusion in light systems.

One of our major accomplishments last year was to develop a systematic understanding of the fusion-fission process in nuclear systems with  $40 \leq A_{cn} \leq 80$ . Based on this work, we are now able to give reliable estimates of the mass and energy dependent cross sections for this process throughout the indicated compound-nucleus mass range. This work also helps clarify the relative significance of dinuclear "orbiting" and fusion-fission in these light systems. A consensus is now emerging, partially resulting from this work, that these are distinct processes, with both contributing in the lighter mass region with  $A_{cn} \approx 40$ . A paper discussing these systematics was prepared and published during the year and is incorporated as part of this progress report.

Another significant accomplishment last year was the completion and beam-line tests of our large-acceptance Bragg-curve detector. This detector is performing as expected and was used in an experimental run using the ATLAS facility towards the end of the year. As outlined elsewhere in this report, we are now continuing our program of detector development by incorporating a position-sensitive, multi-wire proportional counter (MWPC) within the Bragg detector gas enclosure. This hybrid detector will allow energy and nuclear charge determination without the need for a separate transmission detector, with its associated pressure windows, located in front the the Bragg.

Late last year (the week before Christmas) we had a successful run at ATLAS where we obtained a high-resolution Q-value spectrum for the symmetric and near-symmetric fission fragments from the  $^{24}\text{Mg}+^{24}\text{Mg}$  reaction, populating the  $^{48}\text{Cr}$  compound nucleus. This run was motivated in part by our earlier observation of structure in the comparable Q-value spectrum for the  $^{32}\text{S}+^{24}\text{Mg}$  reaction at excitation energies where the number of possible mutual excitations is quite high. Although we have only started looking at our new results, it is already clear that there is a high selectivity in the states populated in the breakup of the  $^{48}\text{Cr}$  system. As part of this measurement we have used our Bragg-curve detector to obtain a better overall view of the fission process in this system. This project also allowed us to start an active collaboration with a group from Sao Paulo, Brazil (headed by A. Szanto de Toledo). We hope to be able to expand our interactions with this group in the future.

Progress was also made during the year on two ongoing analyses. We are close to completing the analysis of our earlier particle-gamma coincidence run studying the symmetric fission of  $^{56}\text{Ni}$  as populated in the  $^{32}\text{S}+^{24}\text{Mg}$  reaction. From this measurement we are learning about the structure of the compound nucleus at scission. The analysis of a fusion-fission measurement in the  $^{29}\text{Si}+^{27}\text{Al}$  system is also nearing completion. With this latter measurement we are interested in determining the fragment mass and nuclear charge dependence of the fusion-fission process for a light, odd-odd system.

During the coming year we expect to complete the analysis of our  $^{32}\text{S}+^{24}\text{Mg}$  particle-gamma run and submit a paper on this work. We also hope to complete the analysis of our  $^{29}\text{Si}+^{27}\text{Al}$  data. Completing the  $^{32}\text{S}+^{24}\text{Mg}$  analysis is particularly timely since we should be able to schedule, finally, a long delayed  $^{40}\text{Ca}+^{16}\text{O}$  particle-gamma coincidence experiment sometime in late spring. This reaction reaches the same  $^{56}\text{Ni}$  compound nucleus as explored with our earlier experiment and the new measurement should help resolve questions concerning the possible role of the entrance channel in our earlier results. Although the  $^{40}\text{Ca}+^{16}\text{O}$  experiment was already approved by the ATLAS PAC at the time of our last annual report, it is only now becoming possible to run the experiment because of the recent radiation safety review at ATLAS.

Although not essential, we hope to have our hybrid MWPC-Bragg curve detector completed by the time we run the  $^{40}\text{Ca}+^{16}\text{O}$  experiment. We already have available the printed circuit boards for this counter's cathode position planes, and the circuit board design for the anode plane is complete and ready to be sent to the PC board manufacturer. If available, the hybrid counter will result in a greater dynamic range for the detected particles in an overall simpler experimental arrangement.

For some time we have been interested in understanding the limits to fusion in light heavy-ion systems. Last year we started to explore the possibility of a measurement which would specifically address the question of nuclear temperature limits to fusion. It is clear that such a measurement has to involve a very mass-asymmetric entrance channel in order to restrict the amount of angular momentum brought into the system. To reach a high nuclear temperature requires a relatively high energy beam. We are still in the process of running Monte Carlo calculations of the fusion-light-particle evaporation process to see if a meaningful measurement is feasible. The principle concern is whether we will be able to distinguish between complete fusion and incomplete fusion processes. Assuming that our simulations indicate a useful experiment is possible, we hope to submit a proposal for this measurement to either the NSCL or IUCL PAC by later this summer.

In the next section we will discuss in more detail the various projects we have been working on during the past year. At the end of this report we have incorporated the cover pages of papers which have appeared in print during the year, but were largely completed previous to this, as well as complete copies of papers completed during the year.

## II. Research Program.

### A. Fusion-fission in light nuclear systems.

When we started our studies of the fusion-fission process in light nuclear systems several years ago, our major goal was to establish the existence of this mechanism and to develop its characteristics. Through a number of studies of the  $^{56}\text{Ni}$  system<sup>1,2,3,4</sup> and studies elsewhere of other light heavy-ion systems<sup>5,6,7</sup> the existence of a light nucleus fusion-fission mechanism is now firmly established. We also have a good understanding of the properties of this mechanism, such as the mass, nuclear charge, and energy dependence of the fragment cross sections, and can show how our current understanding of the macroscopic nuclear potential energy<sup>8</sup> can be used to explain these observations. With the effective shutdown of the ATLAS facility towards the beginning of the year, and the severe restrictions on the type of experiments that could be run later, much of our effort last year was directed towards developing a model calculation that could be used to establish the systematics of compound nucleus fusion-fission in light nuclear systems.<sup>9</sup> In addition to this project, however, we have also made significant progress on the analysis of two experiments where the data acquisition was completed earlier.

#### A.1) Global fission systematics for $40 \leq A_{cn} \leq 80$ .

One of the difficulties facing researchers interested in the fusion-fission process in light systems is the lack of model calculations that can be used to estimate, *a priori*, the magnitude of the associated cross sections. Although the theoretical framework for these calculations in terms of the transition-state model<sup>10</sup> is well established from studies of the fission mechanism in heavier systems, the necessary fission barriers have not been readily available. This is largely because it is essential in these light systems to include finite-nuclear-range and diffuse-

---

<sup>1</sup>S.J. Sanders *et al.*, Phys. Rev. C **34**, 1746(1986).

<sup>2</sup>S.J. Sanders *et al.*, Phys. Rev. Lett. **59**, 2856(1987).

<sup>3</sup>S.J. Sanders *et al.*, Phys. Rev. C **40**, 2091(1989).

<sup>4</sup>S.J. Sanders *et al.*, Phys. Rev. C **41**, R1901(1990).

<sup>5</sup>C. Beck *et al.*, Z. Phys. **A334**, 521(1989).

<sup>6</sup>C. Beck *et al.*, in *Proc. of the Workshop on the Interface Between Nuclear Structure and Heavy-Ion Reaction Dynamics (1990: University of Notre Dame)*, ed. R.R. Betts and J.J. Kolata, (IOP Publishing Ltd., Bristol, 1991), p. 213.

<sup>7</sup>A. Ray *et al.*, Phys. Rev. C **44**, 514(1991).

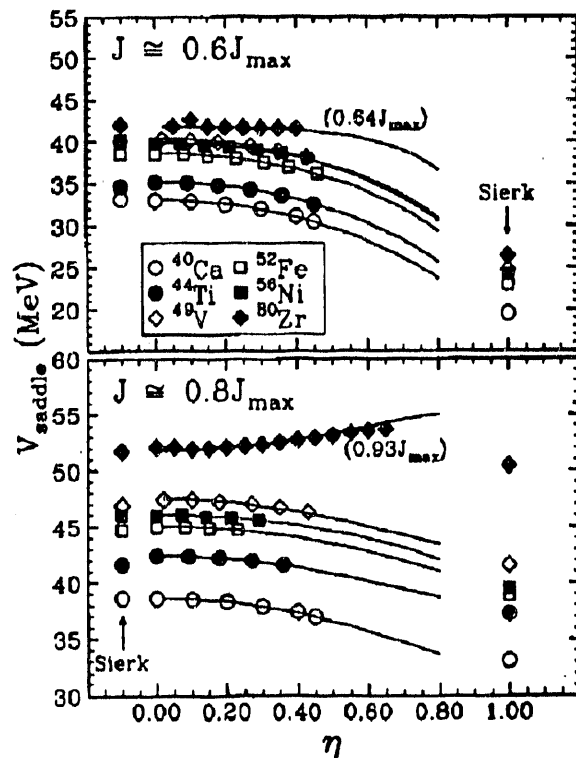
<sup>8</sup>A. Sierk *et al.*, Phys. Rev. C **33**, 2039(1986).

<sup>9</sup>S.J. Sanders, Phys. Rev. C **44**, 2676(1991).

surface effects in calculating the spin and mass asymmetry dependent barriers. Although the procedure for calculating these barriers in terms of the finite-range model (FRM) is straightforward<sup>8</sup>, the calculations are rather time consuming, preventing them from being directly incorporated into transition-state calculations.

To circumvent this problem, we have now devised a simple, double-spheroid model of the saddle-point shape that can be used to quickly and accurately obtain the fission barriers for systems with  $40 \leq A_{cn} \leq 80$ .<sup>9</sup> The parameters for this model are determined by requiring that the FRM fission barriers for a number of systems spanning this mass range be reproduced. In Fig. 1 we show the results of the full macroscopic energy calculations for the mass-asymmetry dependent barrier energies for several different systems by the symbols. The curves in this figure are the results of our double-spheroid approximation. It should be emphasized that a single set of parameters, which has been fitted to the results of the full calculations, is used in these calculations.

Fig. 1 - Fission barrier energies as a function of mass asymmetry for light systems with  $40 \leq A_{cn} \leq 80$ . The two spin values shown for each system correspond to the limits of the spin range where significant fission competition is expected to compete with light-particle emission. The symbols are the results from the full macroscopic energy calculations and the curves are from the double spheroid approximation to these results. The mass asymmetry parameter  $\eta$  is defined by  $\eta = 1 - 2(A_L/A_{cn})$ , where  $A_L$  is the light-fragment mass.



By incorporating the barrier energies obtained through the double-spheroid model into a transition-state fission calculation, we have now been able to compare the predictions of the model with the observed fission-like cross sections throughout the compound-nucleus mass range  $40 \leq A_{cn} \leq 80$ . The calculations are found to do an excellent job in reproducing the

<sup>10</sup>R. Vandenbosch and J.R. Huizenga, *Nuclear Fission*, (Academic Press, New York, 1973).

experimental results, *except for* the data<sup>11,12</sup> for the  $^{40}\text{Ca}$  compound system. It is interesting to note that the experimental results for the  $^{28}\text{Si}+^{14}\text{N}$  reaction,<sup>13</sup> reaching the  $^{42}\text{Sc}$  compound nucleus, *are* well described by our fusion-fission calculations. This leads us to conclude that there most likely is a second mechanism ("orbiting") present in the reactions reaching  $^{40}\text{Ca}$  that accounts in part for the strongly-damped yields observed in this system. The relationship between the fusion-fission, orbiting,<sup>10,11</sup> and molecular resonance behaviors which all seem to coexist in  $^{40}\text{Ca}$  is still unresolved.

A paper on this work was published this year<sup>9</sup> and is bound with this report.

## A.2) Symmetric fission of $^{56}\text{Ni}$ .

The shape of the compound nucleus in its saddle point configuration is expected to be quite deformed. This is seen in Fig. 2 where the saddle-point shapes calculated using the full macroscopic energy calculation (solid curves) are compared to the corresponding shapes of the double-spheroid model (dashed curves) for three systems of different mass asymmetry. Motivated in part by this observation, we have been interested in finding direct evidence for this structural effect by measuring the  $\gamma$ -rays emitted in coincidence with the symmetric fission fragments from  $^{56}\text{Ni}$  decay, as populated using the  $^{32}\text{S}+^{24}\text{Mg}$  reaction. In the breakup process, states in the  $^{28}\text{Si}$  fragments are populated at energies where the level structure is known. By determining which specific mutual excitations are most strongly populated, it is then possible to deduce information about the shape of the system at scission. This measurement was performed using the Argonne-Notre Dame  $\gamma$ -ray facility at ATLAS.

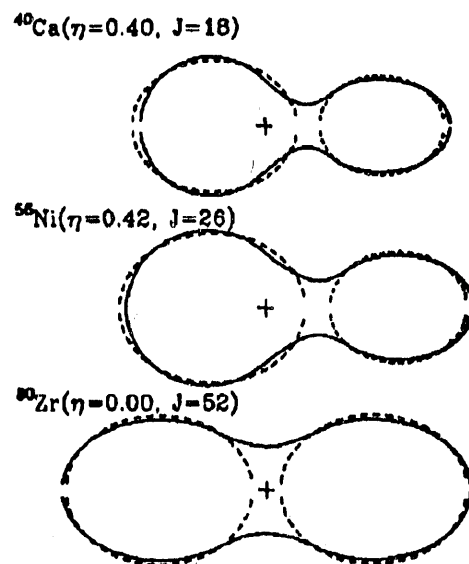
---

<sup>11</sup>D. Shapira *et al.*, Phys. Lett. **114B**, 111(1982).

<sup>12</sup>B. Shivakumar *et al.*, Phys. Rev. C **35**, 1730(1987).

<sup>13</sup>B. Shivakumar *et al.*, Phys. Rev. C **37**, 652(1988).

Fig. 2 – Saddle point shapes calculated using the finite nuclear range model (solid curves) and the corresponding double spheroid approximations to these shapes. The mass asymmetry parameter  $\eta$  is defined in the caption for Fig. 1.



For this measurement the  $^{28}\text{Si}$  fragments from the symmetric fission decay of  $^{56}\text{Ni}$  were detected and identified using a coincidence technique employing two 20cm x 20cm, position-sensitive, multi-wire proportional counters (MWPCs) located on opposite sides of the beam axis. The Q-value for a two-body event is completely determined by the emission angles of the two fragments, after mass identification is first achieved using both position and relative time-of-flight information. One unexpected result that emerged from this measurement, largely because of the very good Q-value resolution possible using this coincidence technique, was the clear observation of structure in the mutual excitation energy spectrum of the two  $^{28}\text{Si}$  fragments even to quite high energy. This is seen in Fig. 3. At the peak of this spectrum, corresponding to a mutual excitation energy of about 13 MeV, the number of possible excitations is on the order of 80/MeV. It is clear that a high degree of selectivity is being exhibited by these results.

We are now in the process of using the coincident  $\gamma$ -ray data obtained during this measurement to firmly establish the specific mutual excitations responsible for the observed structures. The current status of this part of the analysis is indicated by the assignments shown in the Q-value spectrum. This analysis involves determining the population of each of the different possible mutual excitations within the experimental resolution of one of the Q-value peaks such as to reproduce the observed Q-value gated  $\gamma$ -ray spectra, using the summed  $\gamma$ -ray spectrum from the 8 Compton suppressed Ge detectors as well as the  $\gamma$ -ray spectra obtained from the 42 BGO elements surrounding the target. In the figure, where there are several strong mutual excitation responsible for a given peak, the percent of all counts within the indicated Q-value windows that can be attributed to each is indicated. We expect to also be able to assign the dominant excitations responsible for the peak near 16 MeV excitation energy, but at the higher energies the number of possible excitation grows dramatically and the analysis subsequently becomes more difficult. It might be noted that, even though a few mutual

excitations are clearly dominant, the detailed analysis suggests that all possible excitations are excited at some level, typically on the order of 1-5%.

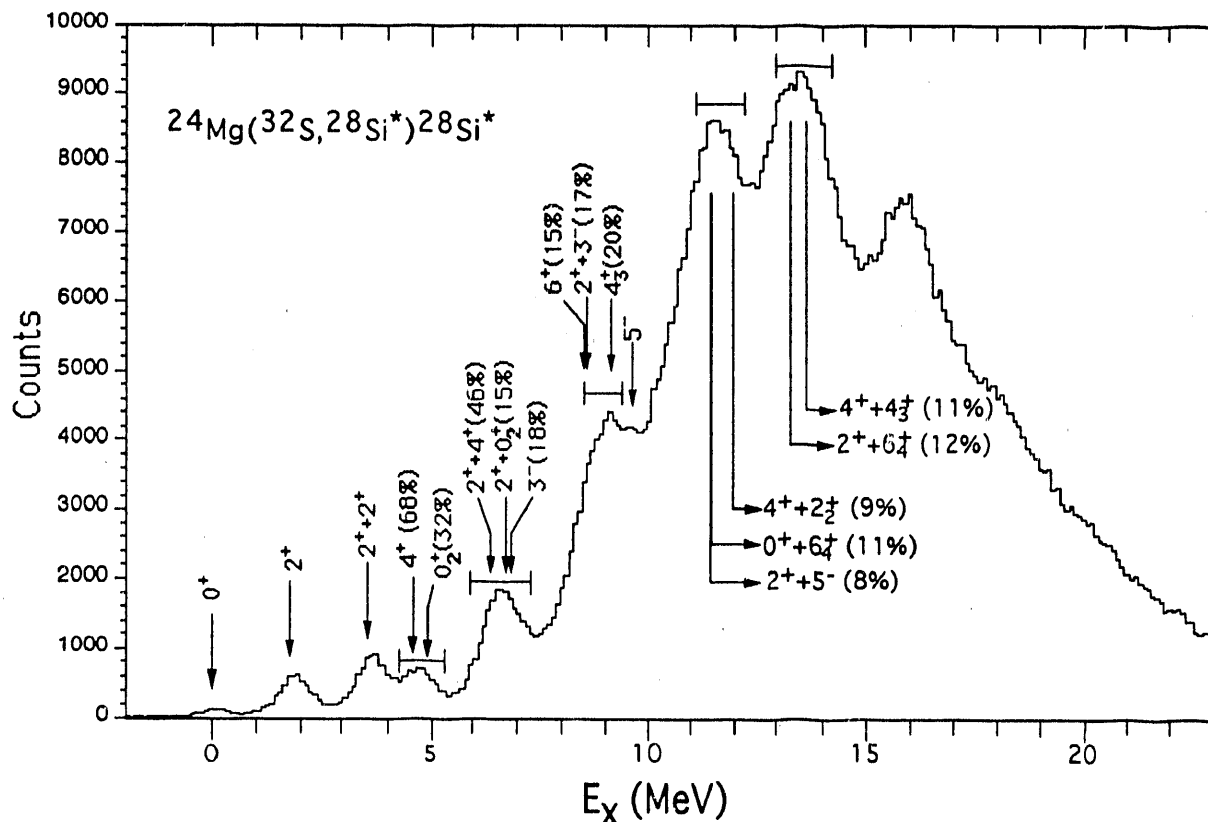


Fig. 3 – Excitation energy spectrum for the  $^{28}\text{Si}$  fragments emitted in the symmetric fission of  $^{56}\text{Ni}$ , as populated with the  $^{32}\text{S}+^{24}\text{Mg}$  reaction at  $E_{\text{lab}}=140\text{MeV}$ . The subscripted, non-yrast, positive parity states are all members of a strongly prolate-deformed band.

The pattern that is emerging from this analysis is very interesting and also somewhat different from what we were expecting based on a preliminary analysis. We knew from an initial analysis of the  $\gamma$ -ray spectrum obtained with an inclusive gate on all  $^{28}\text{Si}$  events that this spectrum was dominated by levels corresponding to the low-lying members of the ground-state band, members of low-lying  $K^\pi=3^-$  and  $5^-$  bands, as well as members of a strongly prolate-deformed, excited  $K^\pi=0^+$  band. Initially it was thought that the strong excitation observed at a 13 MeV excitation energy corresponded to a mutual  $3^-$  excitation. This is now found to be incorrect. The observed structures at high excitation energy seem to be largely dominated by mutual excitations involving the prolate deformed band with members of the ground state band.

We expect to complete the analysis of these data within the next few months. By this summer we hope to have completed the data acquisition stage for the  $^{40}\text{Ca}+^{16}\text{O}$  follow-up experiment. This second experiment will result in significantly better particle- $\gamma$  coincidence statistics and will address the question of a possible entrance-channel dependence for our results.

### A.3) Fusion-fission in the $^{29}\text{Si}+^{27}\text{Al}$ reaction.

One of the striking experimental results that was evident very early in studying the fusion-fission process involving the  $^{56}\text{Ni}$  system was the strong enhancement of the fission yields in the channels involving the even-even,  $N=Z$  nuclei  $^{12}\text{C}$ ,  $^{16}\text{O}$ ,  $^{20}\text{Ne}$ ,  $^{24}\text{Mg}$ , and  $^{28}\text{Si}$ . The dominance of these channels can naively be understood in terms of the strong binding associated with these systems leading to a corresponding lowering of the fission barrier and, hence, a greater fission cross section. In our model calculations of the fusion-fission process in light systems this increased binding is introduced by adjusting the fission barrier by the sum of the Wigner energies of the two nascent fission fragments.

The motivation of our  $^{29}\text{Si}+^{27}\text{Al}$  experiment was to study a light, odd-odd system, also reaching a compound nucleus mass  $A_{\text{CN}}=56$ , where the effect of having two tightly bound fragments in a given breakup channel would not be possible. In addition to measuring the fragment mass distribution, as done in our previous  $^{56}\text{Ni}$  work, in this case the nuclear charge was also determined using an existing Bragg curve detector at the ATLAS facility.<sup>14</sup> Particle-particle coincidences between Si detectors on one side of the beam and a multi-wire proportional counter backed by the Bragg-curve detector on the other established the extent of light-particle evaporation from the fragments.

This past year we have completed the analysis of the particle singles data found using the Si(surface barrier) detectors. These results are shown in Figure 4 together with the corresponding theoretical results based on the calculation discussed earlier. The calculated results include a correction for light-particle emission from the fragments. The general agreement is excellent.

---

<sup>14</sup>M. Vineyard *et al.*, Nucl. Inst. and Meth. A225, 507(1987).

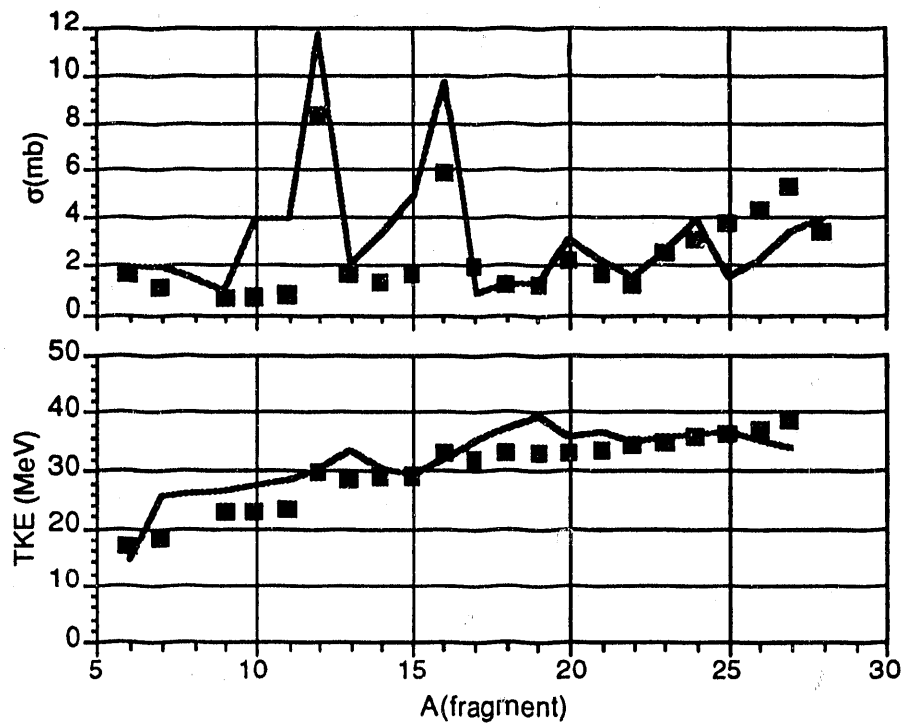


*Fig. 4 – Reaction cross sections (top) and total kinetic energies (bottom) measured for the fusion-fission yields from the  $^{29}\text{Si}+^{27}\text{Al}$  reaction at  $E_{\text{lab}} = 125$  MeV.*

Since obtaining these data, our interest in this experiment has somewhat shifted because of our interim development of a model to calculate fusion-fission cross sections. We expect this  $^{29}\text{Si}+^{27}\text{Al}$  experiment will become the most complete measurement of the detailed mass and charge distribution of the fission process for *any* light system, once the Bragg curve and coincidence data have been analyzed. This should allow us to confront one of the simplifying assumptions of our calculations so as to give a better understanding of the role of nuclear deformation in this process. Currently the fluctuations in mass and charge, which are clearly seen in the data, are introduced in the calculation through the simple Wigner energy term described earlier. Microscopic shell corrections in this mass range should also have a significant (that is, easily measured) influence on the fission yields. Since these shell corrections are also strongly deformation dependent, a careful measurement of the experimental distributions should allow us to deduce these shell corrections and the corresponding deformations.

The most time consuming part of this analysis, involving calibration of the time and energy spectra of the Si(SB) detectors, has been completed. We hope to start analysis of the Bragg curve and corresponding coincidence data shortly and should complete the data reduction by this summer.

## B. High-resolution Q-value measurement for the $^{24}\text{Mg}+^{24}\text{Mg}$ reaction.

As indicated, one of the surprises of our previous particle- $\gamma$  coincidence experiment studying the symmetric fission decay of  $^{56}\text{Ni}$  was the presence of peaks in the Q-value spectra at high excitation energies corresponding to the selective population of certain mutual excitations in the fragments. Motivated by this result, we decided to perform a high-resolution Q-value measurement of  $^{48}\text{Cr}$  fission fragments from the  $^{24}\text{Mg}+^{24}\text{Mg}$  reaction.

The  $^{48}\text{Cr}$  system is interesting for a number of reasons. This system has been predicted to be shell-stabilized in a "hyperdeformed" configuration<sup>15</sup> and strong resonance behavior has been observed in elastic and inelastic scattering measurements of the  $^{24}\text{Mg}+^{24}\text{Mg}$  reaction reaching this system.<sup>16,17</sup> The more symmetric fission channels of  $^{48}\text{Cr}$  have well studied level schemes<sup>18</sup> which facilitates the identification of the stronger mutual excitations—this is in contrast to the situation for  $^{56}\text{Ni}$  fission where the very sketchy information available on the high-spin states of  $^{32}\text{S}$  has hindered our analysis. Further, the  $^{48}\text{Cr}$  system can be populated through a number of reactions now possible at Argonne (including the  $^{36}\text{Ar}+^{12}\text{C}$ ,  $^{16}\text{O}+^{32}\text{S}$ ,  $^{20}\text{Ne}+^{28}\text{Si}$ , and  $^{24}\text{Mg}+^{24}\text{Mg}$  reactions) thus making it possible to easily explore the role of the entrance channel on the breakup of this system.

This measurement using the  $^{24}\text{Mg}+^{24}\text{Mg}$  reaction was completed using the ATLAS facility late last year. The experimental arrangement for the experiment, based in the ATLAS 36" general purpose scattering chamber, is shown in Fig. 5. In this measurement, once the fragments masses are known (using the two positions and relative time of flight information from the two multi-wire proportional counters) the channel Q-value can then be deduced without reference to the timing information, with

$$Q = E_{\text{lab}} \left[ \frac{\frac{A_p \sin^2 \theta_2}{A_1} + \frac{A_p \sin^2 \theta_1}{A_2}}{\sin^2(\theta_1 + \theta_2)} - 1 \right],$$

where  $A_p$  is the projectile mass and  $A_{1(2)}$  and  $\theta_{1(2)}$  are the masses and angles of the two fragments, respectively. The principal contributions to the Q-value resolution then come from multiple-scattering effects in the target, the angular resolution of the MWPCs, and broadening resulting from the emission of  $\gamma$ -rays from the fragments. With a thin target and optimal placement of the counters, a Q-value resolution on the order of a few hundred keV is possible. Since the fusion-fission process has yet to be studied in this system, the measurement also employed the Kansas Bragg-curve detector as well as a number of Si(surface barrier) detectors in order to fully characterize the fusion-evaporation residue and fusion-fission processes.

---

<sup>15</sup>S. Åberg, in *Proceedings of the Copenhagen Workshop – November 1989* (1989).

<sup>16</sup>R.W. Zurmühle *et al.*, *Phys. Lett.* **129B**, 384(1984).

<sup>17</sup>A.H. Wuosmaa *et al.*, *Phys. Rev. C* **41**, 2666(1990).

<sup>18</sup>P.M. Endt, *Nucl. Phys.* **A521**, 1(1990).

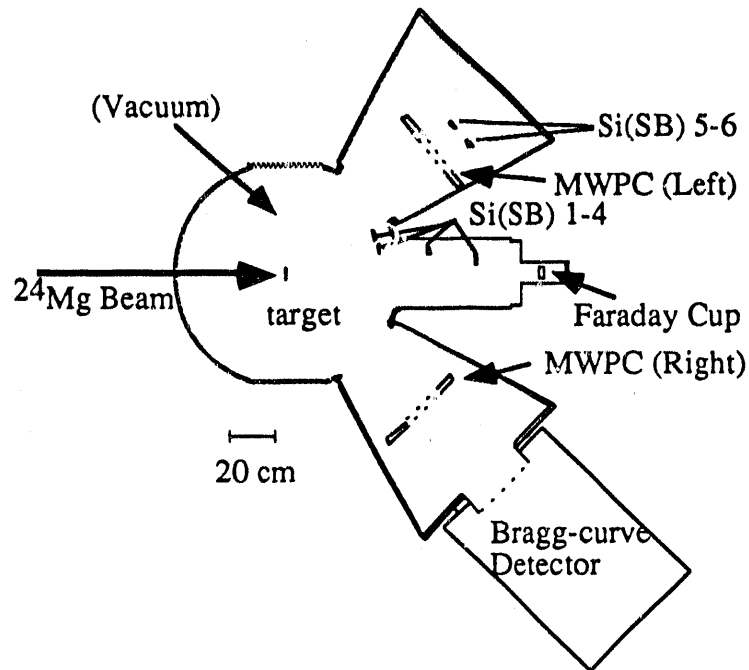


*Fig. 5- Experimental arrangement for the  $^{24}\text{Mg} + ^{24}\text{Mg}$  measurement. The Kansas Bragg-curve detector is behind the right multi-wire proportional counter. A second MWPC is located on the opposite side of the beam to detect the recoiling fragments. Also shown are six Si (surface barrier) detectors used for normalization purposes and to measure the evaporation-residue cross sections. The dashed lines indicate pressure windows. (Drawing is to scale except for target.)*

Although the analysis of this measurement has just begun, Fig. 6 shows the Q-value spectrum achieved on-line for the  $^{24}\text{Mg} + ^{24}\text{Mg}$  channel. (Somewhat improved resolution should be achieved with further analysis.) A high selectivity is found in the mutual excitations populated through the fission process, as previously seen in  $^{56}\text{Ni}$  fission. These initial results are strongly encouraging and suggest that by these studies we may indeed hope to learn about the deformed configurations of this system.

This experiment was done in collaboration with a group from Sao Paulo, Brazil (led by A. Szanto de Toledo) and will form the bases of Ph.D. dissertation for one of our students (A. Hasan).

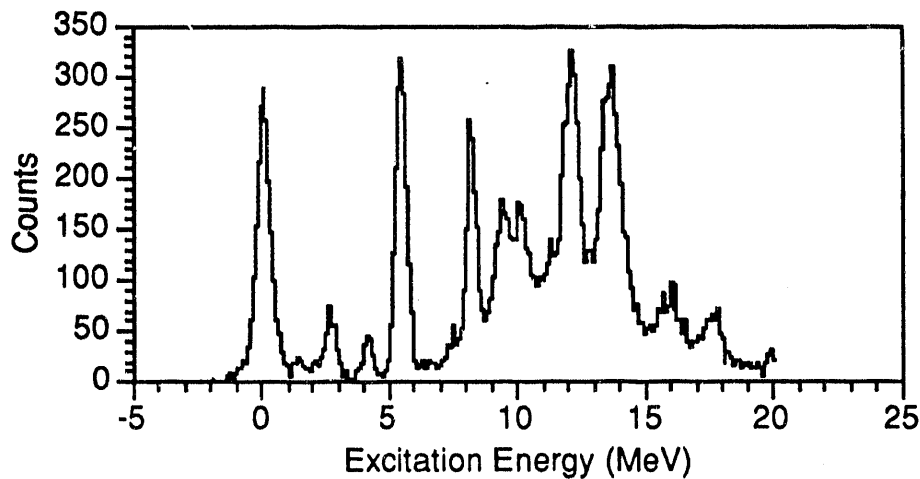


Fig. 6 Spectrum of total excitation energy in  $^{24}\text{Mg}$  fragments from the symmetric fission decay of  $^{48}\text{Cr}$ , as populated in the  $^{24}\text{Mg}+^{24}\text{Mg}$  reaction at  $E_{\text{lab}}=90$  MeV. Note the selective population of states at high excitation energies where numerous excitations are possible.

### C. Heavy-ion reactions and limits to fusion.

In last year's progress report, the possibility of a search for excitation or temperature limitations on fusion was discussed. This will require the use of much more mass-asymmetric systems than we have used before, and the  $^6\text{Li} + ^{51}\text{V}$  system was proposed. The reason for this choice was the availability of  $^6\text{Li}$  beams of high enough energy at NSCL. Some simulations were done using PACE at a beam energy of 150 MeV, as well as some modelling of possible incomplete fusion, with reasonable and encouraging results. However, it was realized that the use of  $^6\text{Li}$  would be undesirable because a large amount of the reaction cross section would be taken up by fragmentation into  $\alpha + d$ , which would also create serious background problems. Since then a  $^4\text{He}^{++}$  beam has been developed at NSCL, which can provide sufficient energy for our purposes. As a result, our more recent simulations have been with the  $^4\text{He} + ^{52}\text{Cr}$  system. The advantages of a mass-asymmetric system are indicated in the following table, where this system is compared to the previous mass 56 systems we have investigated, in each case using the highest energy at which we have obtained data. Here  $l_g$  is the grazing angular momentum and  $l_c$  is the limiting angular momentum calculated from the sharp cutoff approximation for the fusion-evaporation cross section. The limiting angular momentum for fusion<sup>8</sup> is about  $44\hbar$  for mass 56 and it can be seen that all three systems are at or near this value. On the other hand, they are still well below the Morgenstern<sup>19</sup> limitation of  $v_L/c \approx 0.21-0.23$  and the predicted limits on excitation energy and temperature.<sup>20,21</sup>

<sup>19</sup>H. Morgenstern *et al.*, Phys. Rev. Lett. **52**, 1104 (1984).

<sup>20</sup>S. Levit and P. Bonche, Nucl. Phys. **A437**, 426 (1985).

However, the  ${}^4\text{He} + {}^{52}\text{Cr}$  system has already exceeded the Morgenstern limit at 150 MeV and at the higher energies reaches excitation energies and temperatures which may test the Levit limits.

Projectile + Target	$E_{\text{lab}}$ (MeV)	$v_{\text{I}}/c$	$\epsilon^*$ (MeV/A)	T (MeV)	$l_{\text{g}}$ (h)	$l_{\text{c}}$ (h)
${}^{28}\text{Si} + {}^{28}\text{Si}$	452	0.086	4.23	5.82	96.2	32.8
${}^{32}\text{S} + {}^{24}\text{Mg}$	278	0.067	2.38	4.36	48.2	43.9
${}^{16}\text{O} + {}^{40}\text{Ca}$	214	0.110	2.99	4.89	67.8	34.7
${}^4\text{He} + {}^{52}\text{Cr}$	150	0.255	2.62	4.58	35.3	no data
"	300	0.366	5.11	6.39	51.1	"
"	600	0.523	10.08	8.98	73.1	"

The temperature limits predicted in Ref. 21 are shown in the following figure, where it can be seen that  $T \approx 9$  MeV should be ample.

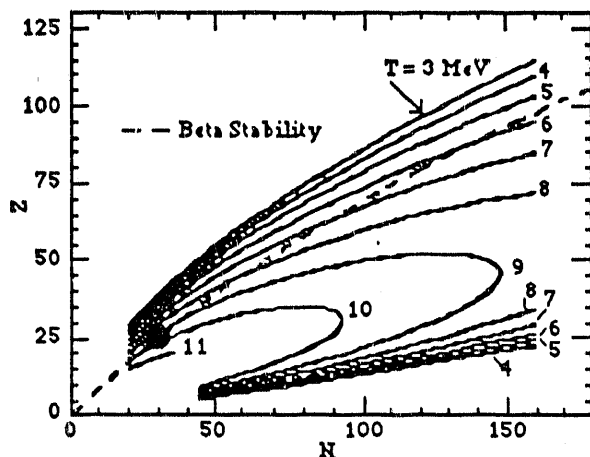


Fig. 7 - Temperature limits on fusion proposed in Ref. 21 shown as a function of proton number  $Z$  and neutron number  $N$  of the fused system. Most systems of interest will lie on or near the indicated line of beta stability. The location of the systems of interest here are indicated by the black dot.

Some typical results of the simulations at 150 MeV are shown below. For comparison, a possible incomplete fusion process might be the pre-equilibrium emission of an  $\alpha$  particle from  ${}^{52}\text{Cr}$ , followed by fusion of the  ${}^4\text{He}$  projectile with the remaining  ${}^{48}\text{Ti}$ . Clearly there is a recognizable shift in both the mass and velocity spectra for at least this incomplete fusion channel. More simulations need to be done of other possible incomplete fusion channels to determine the feasibility of an experiment and the appropriate detector configuration. If the experiment does appear feasible, proposals for beam time at 150 MeV will be submitted to either the NSCL or IUCL PAC (the choice will depend on the final experimental configuration).

<sup>21</sup>J. Besprosvany and S. Levit, Phys. Lett. B 217, 1 (1989).

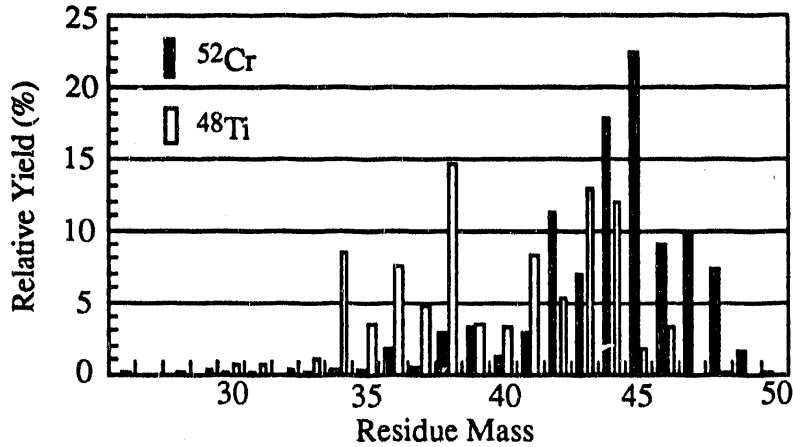


Fig. 8. Simulation of residue mass yields from complete ( $^{52}\text{Cr}$ ) and incomplete ( $^{48}\text{Ti}$ ) fusion using the fusion code PACE.

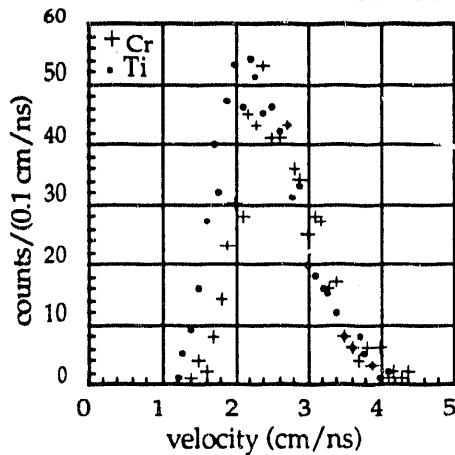
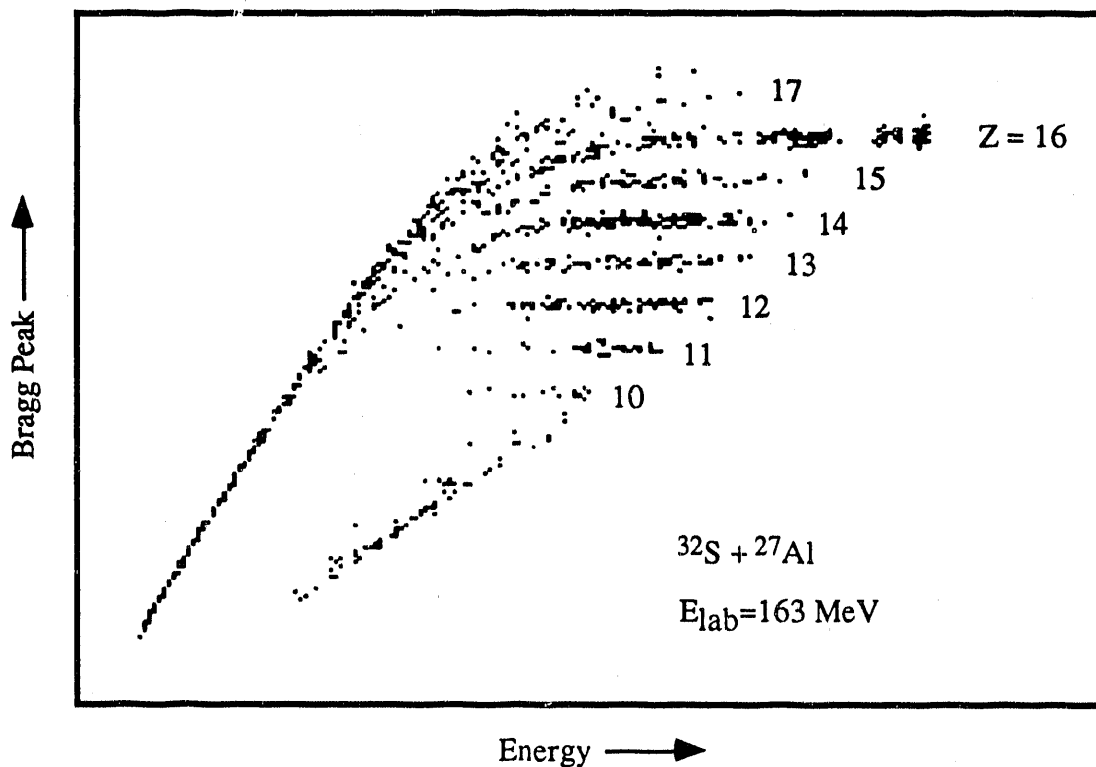


Fig. 9. Comparison of the predicted velocity distributions of  $\alpha$  particles from fusion-evaporation for mass 45 for complete fusion ( $^{52}\text{Cr}$ ) and mass 38 for incomplete fusion ( $^{48}\text{Ti}$ ). In both cases, the  $\alpha$  particles are those in the angular range  $64^\circ - 66^\circ$  relative to the beam direction and in coincidence with residues detected in the range  $20^\circ - 24^\circ$ .

#### D. Hybrid MWPC-Bragg curve detector development .

Last year we completed the development of our large acceptance (12"x12" window opening) Bragg-curve detector. The large acceptance of this detector makes it particularly suitable for particle-gamma coincidence measurements using the BGOSCAT chamber at the Argonne-Notre Dame Gamma-Ray Facility. The Bragg detector yields information about the nuclear charge and total energy of the detected reaction products. In Fig. 10 we show an example of a Bragg peak vs. energy spectrum obtained for the  $^{32}\text{S} + ^{27}\text{Al}$  reaction at  $E_{\text{lab}} = 163$  MeV. Because of its large acceptance, the operation of this detector requires an independent measurement of the angle of incidence of the detected particle. At present this position information is obtained by locating a separate, position-sensitive multi-wire proportional counter MWPC between the target and the Bragg detector. (See Fig. 5.)



*Fig. 8 – Bragg peak vs. energy spectrum obtained using the Kansas Bragg-curve detector. This spectrum corresponds to a restricted solid-angle acceptance. We are currently developing the computer algorithms needed to correct for the dependence of the detector response on the angle of incidence of the detected particle.*

The use of a separate position detector has several disadvantages. The MWPC counter has to be operated in a transmission geometry, requiring the particles to pass through a total of three separate pressure windows, including that for the Bragg. The extra windows associated with the MWPC counter result in a higher energy threshold for particle detection and increase the risk of window failure during a measurement. Also, the MWPC is operated at a much lower pressure than appropriate for the Bragg detector and the requirement of a separate gas handling system increases the complexity of the experimental setup.

Early last year we ran a test using an alpha-particle source to see if reasonable position information could be achieved with a MWPC operated at a pressure comparable to that needed for operation of the Bragg-curve detector. This test showed that increasing the pressure actually improved the position resolution, although at the cost of worsening the timing resolution of the detector. Although good timing is useful for obtaining fragment mass information (using the time structure of the ATLAS beam), for many measurements the identification of nuclear charge, as achieved with the Bragg curve detector, is sufficient. In particular, the trade-off of timing resolution to achieve a simpler experimental configuration with reduced window thickness is reasonable for the light-system particle-gamma

measurements we are currently performing. We are therefore in the process of incorporating a MWPC within our Bragg-curve detector, sharing the common gas volume with the Bragg. A schematic drawing of the overall design is shown in Fig. 9.

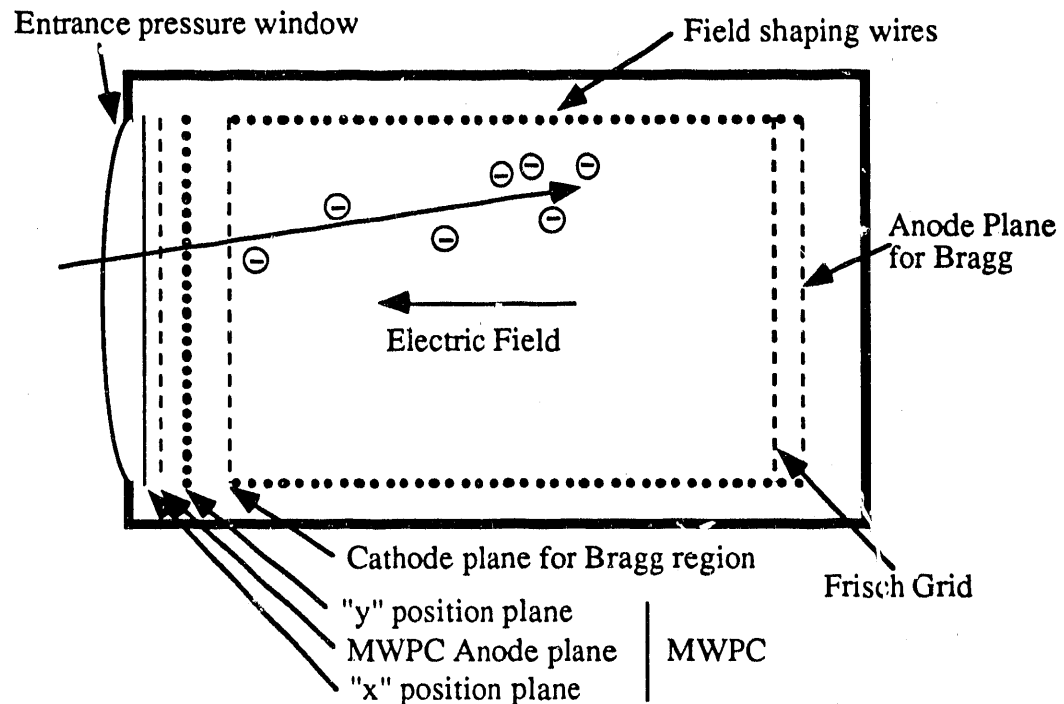


*Fig. 9 Schematic diagram of hybrid MWPC-Bragg curve detector. Electrons released as the incident particle slows down and stops in the counter gas are swept onto the two anode planes. Induced signals on the two position planes determine where the particle enters the counter. This diagram is not to scale. The actual distance between the MWPC anode and each of the position planes is 3mm. The Bragg cathode - Frisch grid distance is 40 cm. The entrance window is 30 cm x 30 cm square.*

The MWPC has been designed and we have achieved delivery of the printed circuit boards for the cathode position planes. We expect to be ready for testing with beam by summer '92 and have had approved by the ATLAS PAC a one day test run for the hybrid detector. If completed in time, we expect to use this detector as part of our upcoming  $^{40}\text{Ca}+^{16}\text{O}$  particle- $\gamma$  coincidence measurement.

### III. Collaborators.

Argonne National Laboratory: B.B. Back, R.R. Betts, M. Freer, D.J. Henderson, R.V.F. Janssens, T.L. Khoo, A.W. Wuosmaa

Sao Paulo, Brazil: A. Szanto de Toledo

### IV. Meetings and Research Trips.

April 22-25 – Washington APS meeting. (Prosser)

May 6-7 – ATLAS: Source test of MWPC at high pressure. (Sanders)

May 15-31 – ATLAS Run: Test of Bragg-curve detector. (Farrar, Hasan, Prosser, and Sanders)

Sept. 11-21 – ATLAS Run: Test of Bragg-curve detector. (Farrar, Hasan, Prosser, and Sanders)

Oct. 24-26 – Fall APS Nuclear Divisional Meeting. (Sanders, Prosser)

Dec. 6 – ATLAS Open PAC meeting. (Sanders: "Particle- $\gamma$  coincidence experiments at ATLAS")

Dec. 10-21 – ATLAS Run: High resolution Q-value measurement of  $^{24}\text{Mg}+^{24}\text{Mg}$  fusion-fission. (Hasan, Farrar, Prosser, Sanders).

(Note: For the ATLAS runs the entire group would, in general, not be present for the full time indicated.)

### V. Personnel.

Senior personnel:

Francis W. Prosser    Professor of Physics

Stephen J. Sanders    Associate Professor of Physics

Graduate Students:

Kelly Farrar

Asad Hasan

Zhou Dacheng

**END**

**DATE  
FILMED**

**8 / 11 / 92**

